

**This is an electronic reprint of the original article.
This reprint *may differ* from the original in pagination and typographic detail.**

Author(s): McCrea-Hendrick, Madison L.; Caputo, Christine A.; Roberts, Christopher; Fettinger, James C.; Tuononen, Heikki; Power, Philip P.

Title: Reactions of Terphenyl-Substituted Digallene AriPr₄GaGaAriPr₄ (AriPr₄ = C₆H₃-2,6-(C₆H₃-2,6-iPr₂)₂) with Transition Metal Carbonyls and Theoretical Investigation of the Mechanism of Addition

Year: 2016

Version:

Please cite the original version:

McCrea-Hendrick, M. L., Caputo, C. A., Roberts, C., Fettinger, J. C., Tuononen, H., & Power, P. P. (2016). Reactions of Terphenyl-Substituted Digallene AriPr₄GaGaAriPr₄ (AriPr₄ = C₆H₃-2,6-(C₆H₃-2,6-iPr₂)₂) with Transition Metal Carbonyls and Theoretical Investigation of the Mechanism of Addition. *Organometallics*, 35(4), 579-586.
<https://doi.org/10.1021/acs.organomet.5b00992>

All material supplied via JYX is protected by copyright and other intellectual property rights, and duplication or sale of all or part of any of the repository collections is not permitted, except that material may be duplicated by you for your research use or educational purposes in electronic or print form. You must obtain permission for any other use. Electronic or print copies may not be offered, whether for sale or otherwise to anyone who is not an authorised user.

Reactions of Terphenyl Substituted Digallene $\text{Ar}^{i\text{Pr}_4}\text{GaGaAr}^{i\text{Pr}_4}$ ($\text{Ar}^{i\text{Pr}_4} = \text{C}_6\text{H}_3\text{-2,6-(C}_6\text{H}_3\text{-2,6-}^i\text{Pr}_2)_2$) with Transition Metal Carbonyls and Theoretical Investigation of the Mechanism of Addition

Madison L. McCrea-Hendrick,¹ Christine A. Caputo,^{1†} Christopher J. Roberts,² James C. Fettinger,¹ Heikki M. Tuononen,^{2*} Philip P. Power^{1*}

¹ Department of Chemistry, The University of California Davis, 1 Shields Ave., Davis, CA, USA. Tel: 1-530-752-8900; Fax: 1-530-732-8995; E-mail: pppower@ucdavis.edu.

² University of Jyväskylä Department of Chemistry, Nanoscience Center, P.O. Box 35, FI-40014 University of Jyväskylä, Finland. E-mail: heikki.m.tuononen@jyu.fi.

†Present Address: Department of Chemistry, The University of New Hampshire, Durham, NH, USA 03824

KEYWORDS: gallium, low coordinate, group 13, terphenyl ligand, transition metal carbonyl, clusters, density functional theory calculations, reaction mechanism

ABSTRACT

The neutral digallene $\text{Ar}^{i\text{Pr}_4}\text{GaGaAr}^{i\text{Pr}_4}$ ($\text{Ar}^{i\text{Pr}_4} = \text{C}_6\text{H}_3\text{-2,6-(C}_6\text{H}_3\text{-2,6-}^i\text{Pr}_2)_2$) was shown to react at *ca.* 25°C in pentane solution with group 6 transition metal carbonyl complexes $\text{M}(\text{CO})_6$ ($\text{M} = \text{Cr, Mo, W}$) under UV irradiation to afford compounds of the general formula *trans*- $[\text{M}(\text{GaAr}^{i\text{Pr}_4})_2(\text{CO})_4]$ in modest yields. The bis(gallanediyl) complexes were characterized spectroscopically and by X-ray crystallography, which demonstrated that they were isostructural. In each complex, the gallium atom is two-coordinate with essentially linear geometry, which is relatively rare for gallanediyl substituted transition metal species. The experimental data show that the gallanediyl ligand $:\text{GaAr}^{i\text{Pr}_4}$ behaves as a good σ -donor but a poor π -acceptor, in agreement with prior theoretical analyses on related systems. In addition, the monogallanediyl complex $\text{Mo}(\text{GaAr}^{i\text{Pr}_4})(\text{CO})_5$ was synthesized by reacting $\text{Ar}^{i\text{Pr}_4}\text{GaGaAr}^{i\text{Pr}_4}$ with two equivalents of $\text{Mo}(\text{CO})_5\text{NMe}_3$ in THF solution. The mechanism of the reaction between $\text{Ar}^{i\text{Pr}_4}\text{GaGaAr}^{i\text{Pr}_4}$ and $\text{Cr}(\text{CO})_6$ was probed computationally using density functional theory. The results suggest that the reaction proceeds via an intermediate monogallanediyl complex $\text{Cr}(\text{GaAr}^{i\text{Pr}_4})(\text{CO})_5$ that can be generated via two pathways, one of which involves the dimeric $\text{Ar}^{i\text{Pr}_4}\text{GaGaAr}^{i\text{Pr}_4}$, that are possibly competing. $\text{Ar}^{i\text{Pr}_4}\text{GaGaAr}^{i\text{Pr}_4}$ was also shown to react readily under ambient conditions with $\text{Co}_2(\text{CO})_8$ to give the monosubstituted dicobalt complex $\text{Co}_2(\mu\text{-GaAr}^{i\text{Pr}_4})(\mu\text{-CO})(\text{CO})_6$ by X-ray crystallography. The $:\text{GaAr}^{i\text{Pr}_4}$ unit bridges the Co–Co bond unsymmetrically in the solid state. No evidence was found for incorporation of more than one $:\text{GaAr}^{i\text{Pr}_4}$ unit into the dicobalt complex.

INTRODUCTION

Recent investigations have demonstrated the ability of digallenes to act as heavy element alkene analogues,¹ and despite being in equilibrium with its dissociated monomer *i.e.* gallanediyl $:GaAr^{iPr_4}$,² they were shown to react in their dimeric digallene $Ar^{iPr_4}GaGaAr^{iPr_4}$ form. They undergo cycloaddition with simple olefins (*e.g.* ethylene, propene, styrene, 1-hexene)³ and cyclic polyolefins (*e.g.* norbornadiene, cyclooctatetraene, cycloheptatriene and cyclopentadiene) in a manner that is directed by frontier orbital symmetry.⁴ Although the reactions of the digallene proceeded in a similar manner to their alkene counterparts, they reacted much more rapidly than alkenes under ambient conditions and without the use of transition metal catalysts. The increased reactivity is due to differences in the frontier orbital symmetries of the two species: the HOMO and LUMO of *cis*-digallene have the correct symmetry and shape to react with the LUMO and HOMO of the alkenes.^{1,5}

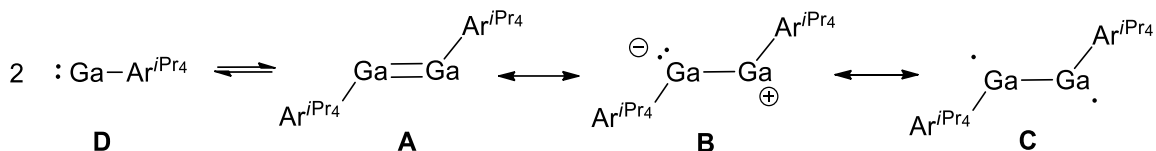


Figure 1. Resonance forms of $Ar^{iPr_4}GaGaAr^{iPr_4}$ (**A**, **B** and **C**) in equilibrium with the monomeric gallanediyl (**D**).

The bonding in digallenes can be thought of in terms of three primary resonance forms, **A** to **C** (Figure 1).⁶ We have shown previously, by calculation and by analysis of electronic spectra and melting point depression experiments, that for derivatives of the ligand Ar^{iPr_4} ($Ar^{iPr_4} = C_6H_3-2,6-(C_6H_3-2,6-*i*Pr_2)_2$), an equilibrium exists between **A** and **D** in hydrocarbon solutions.^{2c} With a sufficiently bulky ligand, however, the monomeric form **D** can be favored even in the solid state and a stable example, $:GaAr^{iPr_8}$ ($Ar^{iPr_8} = C_6H-2,6-(C_6H_3-2,6-*i*Pr_2)_2-3,5-*i*Pr_2$), has been structurally characterized using X-ray crystallography.² It may also be possible to stabilize the resonance form **B** by addition of an appropriate Lewis acid, though this has yet to be proven. However, Rivard and coworkers have shown that heavier group 14 element analogues of ethylene related to **B** are isolable when stabilized by both a Lewis acid and a base.⁷ On the other hand, high-level theoretical

analyses have shown that even though the diradical structure **C** is required for an accurate representation of the electronic structure of digallenes, it does not seem to dictate the chemistry they undergo.⁶

Because of the presence of the lone pair and two empty p-orbitals at gallium in the monomeric gallanediyl **D**, low-coordinate Ga^IR species have been considered as isolobal analogues of CO.⁸ However, unlike CO, they behave predominantly as σ -donor ligands. The poor π -acceptor nature of GaR has been corroborated by Frenking and coworkers with theoretical calculations.⁹ Jutzi and coworkers have previously shown that GaCp* (Cp* = η^5 -pentamethylcyclopentadienyl) forms complexes with transition metal carbonyls to give both monosubstituted and bridged products such as Cr(GaCp*)(CO)₅ (**II-Cr**), Fe(GaCp*)(CO)₄, Co₂(μ -GaCp*)₂(CO)₆ (**VI-Co**) and Fe₂(μ -GaCp*)₃(CO)₆ (**VII**) (Figure 2).¹⁰ The trisubstituted metal complexes *fac*-[M(GaCp*)₃(CO)₃] (**III-Mo** and **III-W**) have been isolated by Fischer and coworkers.¹¹

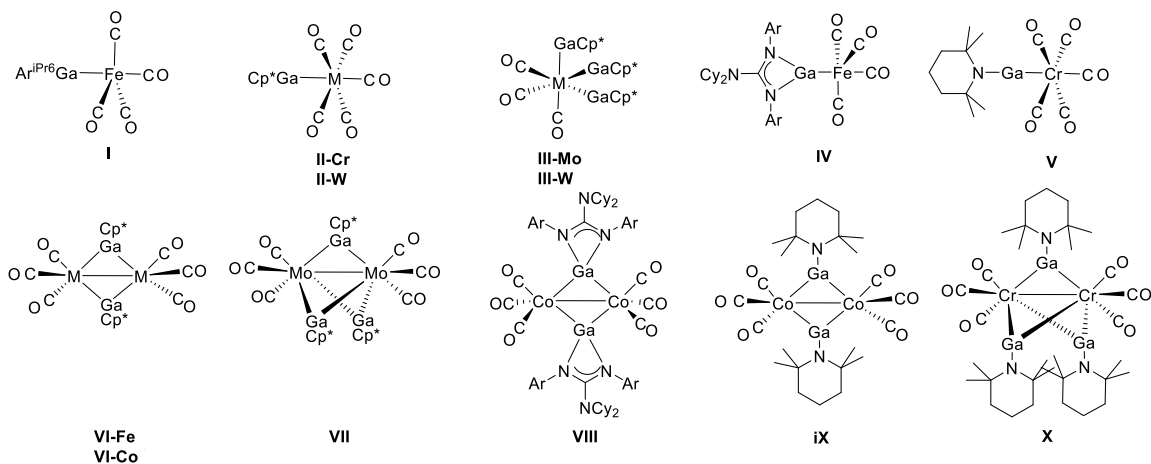
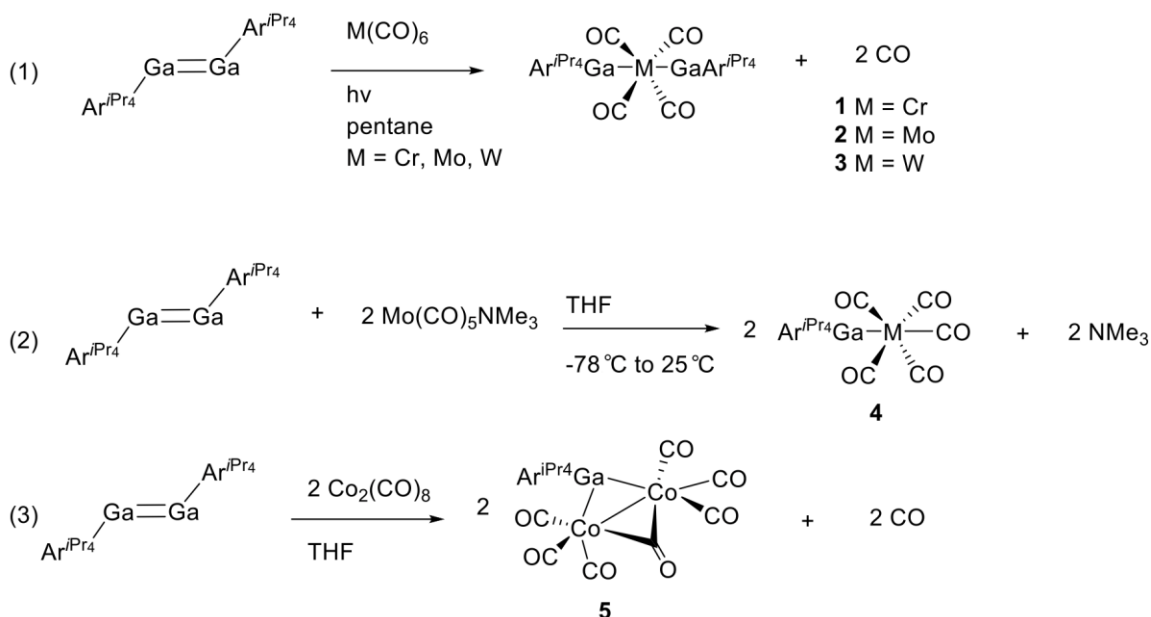


Figure 2. Some known gallanediyl complexes of group 6, 7 and 8 transition metal carbonyls.

The only gallanediyl transition metal carbonyls in which gallium is two-coordinate have been reported by groups of Linti and Robinson: Linti and coworkers have shown that a 2,2,6,6-tetramethylpiperidino (tmp) stabilized Ga(I) species reacts with transition metal carbonyls to form complexes Cr{Ga(tmp)}(CO)₅ (**V**) and Co₂{ μ -Ga(tmp)}₂(CO)₆ (**IX**),¹² whereas Robinson and coworkers synthesized Fe(GaAr^{tPr6})(CO)₄ (**I**) via salt metathesis

between $\text{Na}_2[\text{Fe}(\text{CO})_4]$ and $\text{Ar}^{i\text{Pr}_4}\text{GaCl}_2$ ($\text{Ar}^{i\text{Pr}_4} = \text{C}_6\text{H}_3\text{-}2,6\text{-(C}_6\text{H}_2\text{-}2,4\text{-}6\text{-}i\text{Pr}_3)_2$).¹³ Other published examples of mono and bis(gallenediyl) complexes include those by Jones and coworkers which feature bonds between gallium analogues of *N*-heterocyclic carbenes and a variety of transition metal species, including several carbonyl complexes (**IV** and **VIII**).¹⁴ A number of gallenediyl complexes of group 10 carbonyls such as $\text{Ni}_4(\text{GaAr}^{i\text{Pr}_4})_3(\text{CO})_7$, $\text{Ni}(\text{GaL})(\text{CO})_3$ and $\text{Ni}(\text{GaL})_2(\text{CO})_2$ ($\text{L} = \text{HC}[\text{C}(\text{Me})\text{N}(\text{C}_6\text{H}_3\text{-}2,6\text{-}i\text{Pr}_2)]_2$) have also been reported.¹⁵



Scheme 1. Reactions of $\text{Ar}^{i\text{Pr}_4}\text{GaGaAr}^{i\text{Pr}_4}$ with transition metal carbonyl complexes to form **1–5**.

In this contribution, we show that the low-coordinate digallene $\text{Ar}^{i\text{Pr}_4}\text{GaGaAr}^{i\text{Pr}_4}$ undergoes reactions with transition metal carbonyl compounds (Scheme 1). The reaction of the neutral group 6 metal carbonyls $\text{M}(\text{CO})_6$ and dimeric $\text{Ar}^{i\text{Pr}_4}\text{GaGaAr}^{i\text{Pr}_4}$ gives disubstituted transition metal complexes *trans*- $[\text{M}(\text{GaAr}^{i\text{Pr}_4})_2(\text{CO})_4]$, $\text{M} = \text{Cr}$ (**1**), Mo (**2**) and W (**3**). Density functional theory calculations conducted for $\text{Ar}^{i\text{Pr}_4}\text{GaGaAr}^{i\text{Pr}_4}$ and $\text{Cr}(\text{CO})_6$ indicate that this reaction most likely proceeds via the monosubstituted intermediate $\text{Cr}(\text{GaAr}^{i\text{Pr}_4})(\text{CO})_5$ in which the Ga–Ga bond has been broken as a result of the interaction with the photochemically generated $\text{M}(\text{CO})_5$. This intermediate can form by the direct reaction of $\text{Cr}(\text{CO})_5$ with $:\text{GaAr}^{i\text{Pr}_4}$ or by coordination of $\text{Cr}(\text{CO})_5$ to

$\text{Ar}^{i\text{Pr}_4}\text{GaGaAr}^{i\text{Pr}_4}$, followed by simultaneous cleavage of the Ga–Ga bond. We show here that the molybdenum congener $\text{Mo}(\text{GaAr}^{i\text{Pr}_4})(\text{CO})_5$ (**4**) can be isolated from the reaction of $\text{Ar}^{i\text{Pr}_4}\text{GaGaAr}^{i\text{Pr}_4}$ with $\text{Mo}(\text{NMe}_3)(\text{CO})_5$. The digallene $\text{Ar}^{i\text{Pr}_4}\text{GaGaAr}^{i\text{Pr}_4}$ is also shown to react with $\text{Co}_2(\text{CO})_8$ to form $\text{Co}_2(\mu\text{-GaAr}^{i\text{Pr}_4})(\mu\text{-CO})(\text{CO})_6$ (**5**).

RESULTS AND DISCUSSION

Structures. The complexes **1–3** were prepared by dissolving digallene $\text{Ar}^{i\text{Pr}_4}\text{GaGaAr}^{i\text{Pr}_4}$ in pentane in a quartz Schlenk flask and adding 1 equivalent of $\text{M}(\text{CO})_6$, $\text{M} = \text{Cr}, \text{Mo}, \text{W}$. The solution was then irradiated with UV light for 2–24 hours, during which time the mixture changed from dark green to either red or yellow. Concentration and cooling of the solution gave X-ray quality crystals and an additional crop of crystals could be isolated by storing the concentrated solution at $-18\text{ }^\circ\text{C}$. In all cases, the yields of the isolated complexes were modest. Attempts to increase the yield by using different solvents or prolonged reaction times were unsuccessful. This may be due to increased decomposition of either the digallene or the group 6 transition metal hexacarbonyls under prolonged exposure to UV irradiation.

The ^1H NMR spectroscopic data for **1–3** highlight the symmetric nature of the complexes in solution: in all cases the NMR spectra displayed signals due to only one Ar^{iPr_4} environment. The ^1H NMR data of **1–3** are also almost identical between different complexes with only very slight chemical shift changes being observed. This is to be expected as all protons are significantly distant in space from the transition metal center. The $^{13}\text{C}\{^1\text{H}\}$ NMR chemical shift of the carbonyl signal in **1–3** moves upfield as the group is descended: 220.5, 211.0 and 196.2 ppm for the Cr, Mo and W complexes, respectively. These values show a similar trend to the $^{13}\text{C}\{^1\text{H}\}$ NMR chemical shifts of the analogous hexacarbonyls $\text{M}(\text{CO})_6$,¹⁶ whose electronic structures have been analyzed by Ziegler and coworkers.¹⁷ They observed that within the group 6 triad, the chemical shift decreases as σ -donation becomes more important for the heavier congeners due to relativistic effects.

The solid-state structures of **1–3** are illustrated in Figure 3 with selected bond distances and angles presented in Table 1. Each complex crystallizes in the monoclinic

space group $C2/c$. The unit cells of complexes **1–3** contain two crystallographically independent molecules of which only one molecule from each structure is shown in Figure 3. In all cases the coordination sphere of the transition metal atom is six-coordinate with the two $:GaAr^{iPr_4}$ ligands in axial positions. The *trans*-orientation of the gallanediyl ligands in **1–3** is consistent with the minimization of steric crowding produced by the bulky terphenyl substituents. The steric bulk of the flanking diisopropylphenyl rings is likely also the reason why the central aryl rings of the terphenyl ligands in **1–3** are not coplanar in the solid state but have torsion angles that vary from $-34.5(1)$ to $-36.2(4)^\circ$. However, the solution 1H NMR data indicates that the barrier for the rotation of the central aryl rings in **1–3** is rather small as all Ar^{iPr_4} groups were found to be equivalent on the NMR timescale.

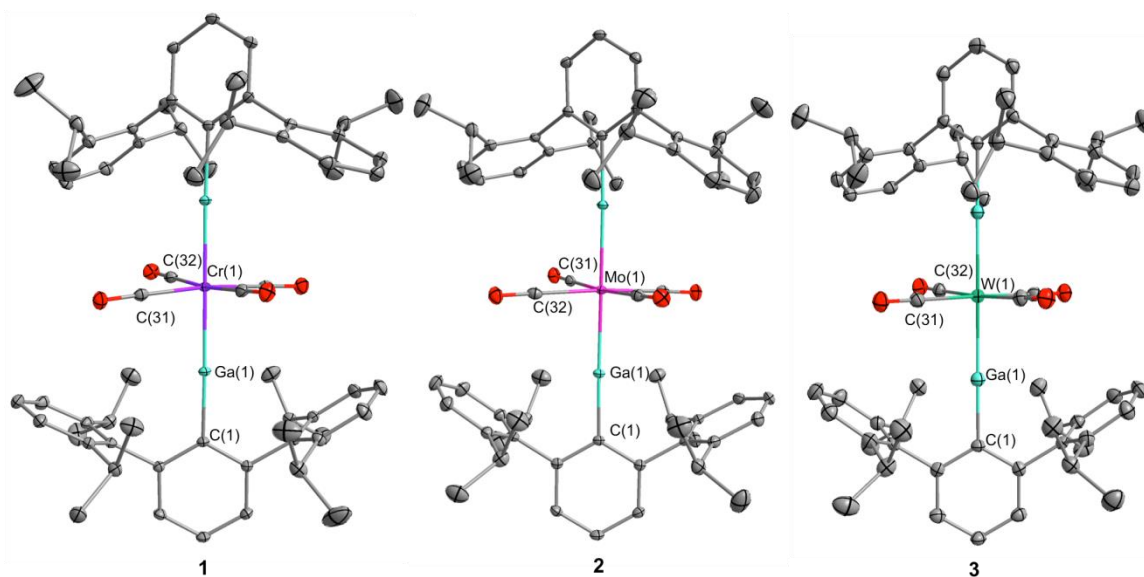


Figure 3. Thermal ellipsoid (50 %) plots of complexes **1–3** with hydrogen atoms omitted for clarity. Only one crystallographically independent molecule is shown.

Compound **4** was synthesized by reacting $Ar^{iPr_4}GaGaAr^{iPr_4}$ with two equivalents of $Mo(CO)_5NMe_3$ in THF at *ca.* $-78^\circ C$. Compound **4** crystallizes in the monoclinic space group $P2_1/c$ and its molecular structure is depicted in Figure 4 and selected bond lengths and angles given in the figure legend and in Table 1. The unit cell contains two molecules, one of which has disorder in three of the four carbonyl ligands. For clarity, the molecule without disorder is shown in Figure 4. The C–O bond length in the carbonyl ligand *trans* to the aryl gallanediyl moiety is $2.032(2)$ Å [$2.0270(19)$ Å] which is shorter than those to

the carbonyl atoms in the equatorial plane by *ca.* 0.009–0.021 Å. The σ -donor properties of the gallanediyl ligand increase the electron density on molybdenum, which enhances π -interactions with the carbonyl *trans* to the gallanediyl and thereby shortens the Mo–CO bond length.

Table 1. Selected Bond Distances (Å) and Angles (°) for Structures **1–4**.^a

Compound	Ga–M	Ga–C _{ipso}	Ga–M–Ga	Ar...Ar torsion
1 (M = Cr)	2.3136(3)	1.978(7)	179.21(11)	–34.5(1)
2 (M = Mo)	2.4562(5)	1.977(2)	178.05(3)	–36.0(1)
3 (M = W)	2.4572(4)	1.974(3)	179.179(2)	–36.2(4)
4 (M = Mo)	2.4928(5)	1.9634(17)	N/A	N/A

^a Bond distances and angles are reported for only one crystallographically independent molecule in the unit cell.

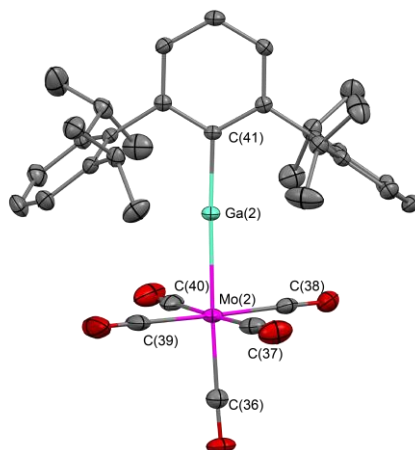


Figure 4: Thermal ellipsoid (50 %) plot of complex **4**. Hydrogen atoms are omitted for clarity. Only one crystallographically independent molecule is shown. Selected bond lengths (Å) and angles (°): C(41)–Ga(2) 1.9634(17); Ga(2)–Mo(2) 2.4928(5); Mo(2)–C(36) 2.032(2); Mo(2)–C(37) 2.044(2); Mo(2)–C(38) 2.041(2); Mo(2)–C(39) 2.047(2); Mo(2)–C(40) 2.053(2); C(41)–Ga(2)–Mo(2) 177.49(5); Ga(2)–Mo(2)–C(36) 177.75(6); Ga(2)–Mo(2)–C(37) 89.60(6); Ga(2)–Mo(2)–C(38) 88.53(5); Ga(2)–Mo(2)–C(39) 89.85(6); Ga(2)–Mo(2)–C(40) 88.67(6).

Structures **1–4** are rare examples^{12,13} of transition metal complexes where gallium is two-coordinate and the first reported instances of bis(gallanediyl) complexes of group 6 elements. The M–Ga–C units in **1–4** are nearly linear with Ga–M bond distances for **1–3** and a Ga–Mo bond distance for **4**, that are significantly shorter than the sum of the Pyykkö-Atsumi single-bond covalent radii for the respective elements:¹⁸ Ga–Cr, 2.3136(3), 2.3083(7) and 2.3186(7) vs. the predicted 2.46 Å for **1**; Ga–Mo, 2.4562(5), 2.4544(5) and 2.4637(5) vs. 2.62 Å for **2**; and Ga–W, 2.4572(4), 2.4536(6) and 2.4623(6) vs. 2.61 Å for **3**; and 2.4928(5) and 2.5003(5) vs. 2.62 Å for **4**. These differences are not necessarily indicative of strong back-bonding interactions but can be rationalized in terms of the high 4s character of the gallium lone pair, which significantly reduces the spatial extent of the donor orbital (the effective radii of Ga 4s and 4p orbitals are 1.06 and 1.40 Å, respectively).¹⁹ Accordingly, the calculated Wiberg bond indices for Ga–M in **1–3** span a narrow range from 0.78 to 0.81. The Ga–C_{ipso} distances in **1–4** (1.9634(17)–1.978(7) Å) are slightly shorter than the Ga–C_{ipso} distance in the monomer :GaAr^{iPr₃} (2.03(1) Å) and in the dimer Ar^{iPr₄}GaGaAr^{iPr₄} (2.025(3) Å).² The shortening of the bond can be explained by the removal of electron density from gallium to the transition metal by σ -donation, which increases the partial positive charge on gallium and therefore the degree of Ga–C attraction.

The IR spectra of **1–3** display a single strong CO stretching band whose frequency increases down the group with increasing atomic number (Cr(CO)₄ 1894 cm⁻¹; Mo(CO)₄ 1904 cm⁻¹; W(CO)₄ 1928 cm⁻¹). These values resemble the pattern shown by *trans*-bis(phosphine) metal carbonyls, which were studied by Poilblanc and coworkers and also showed a single CO stretching band near this range (*e.g.* 1881 and 1885 cm⁻¹ for *trans*-[M{P(CH₃)₃]₂(CO)₄] (M = Cr or W)) suggesting that the gallanediyl ligand is a marginally better π -acceptor ligand than a trialkylphosphine.²⁰ The CO stretching frequencies in **1–3** are *ca.* 100 cm⁻¹ lower than those of the corresponding hexacarbonyls M(CO)₆, all of which show a single intense band near 2000 cm⁻¹ in the gas phase. This suggests that the two :GaAr^{iPr₄} ligands in **1–3** engage in very weak π -back-bonding interactions, for which reason the *d*-electron flow from the central metal to the π^* orbitals of the carbonyl ligands is increased in comparison to the corresponding hexacarbonyls. Bonding and back-bonding interactions in transition metal complexes with terminal group-13 diyl ligands have been analyzed theoretically by Uddin and Frenking.⁹

The cobalt complex **5** was synthesized in a similar manner to **1–3** but with use of THF as the solvent. The solid-state structure of **5** is illustrated in Figure 5 with selected bond distances and angles provided in the figure legend. This complex can be described as a derivative of the $\text{Co}_2(\text{CO})_8$ dimer in which one of the bridging CO molecules is replaced with a $:\text{GaAr}^{i\text{Pr}_4}$ ligand, $\text{Co}_2(\mu\text{-GaAr}^{i\text{Pr}_4})(\mu\text{-CO})(\text{CO})_6$. The remaining terminal carbonyl ligands are found in a slightly staggered conformation with a $\text{C}(1)\text{-Co}(1)\text{-Co}(2)\text{-C}(8)$ torsional angle of 10.58° . The $:\text{GaAr}^{i\text{Pr}_4}$ unit bridges the Co–Co bond unsymmetrically, causing the Ga atom to be significantly closer to one of the two Co centers $\text{Ga}(1)\text{-Co}(1)$ 2.3891(3) Å and $\text{Ga}(1)\text{-Co}(2)$ 2.3366(3) Å. The bridging CO ligand is also bound unsymmetrically ($\text{Co}(1)\text{-C}(4)$ 1.9130(2) and $\text{Co}(2)\text{-C}(4)$ 1.930(2) Å). The observed asymmetry can be attributed to the steric influence of the terphenyl ligand, which may also be the reason for the incorporation of only one $:\text{GaAr}^{i\text{Pr}_4}$ moiety. These results are in contrast to the analogous reactions carried out by Jutzi and coworkers, who found that GaCp^* units could substitute both bridging CO groups to form a C_2 symmetric complex.¹⁰ Disubstitution was also seen by Seifert and Linti, who successfully formed $\text{Co}_2\{\text{Ga}(\text{tmp})\}_2(\text{CO})_6$ with symmetrically bridging $\text{Ga}(\text{tmp})$ ligands.¹² The Co–Co bond length in **5** (2.5802(4) Å) is elongated in comparison to that in $\text{Co}_2(\text{CO})_8$ (2.5301(8) Å and 2.5278(8) Å)²¹ and $\text{Co}_2(\mu\text{-GaCp}^*)_2(\text{CO})_6$ (2.3784(5)–2.3959(5) Å),¹⁰ but is shorter than those in $\text{Co}_2\{\text{Ga}(\text{tmp})\}_2(\text{CO})_6$ (2.836(1) Å)¹² and in the closely related carbene complex $\text{Co}_2(\mu\text{-GaG}_{\text{iso}})_2(\text{CO})_6$ (2.7725(9) Å, $\text{G}_{\text{iso}} = [\{\text{N}(\text{Ar})\}_2\text{CN}(\text{C}_6\text{H}_{11})_2]^-$).^{14a} The $\text{Ga}(1)\text{-C}(9)$ bond length to the ipso carbon of the terphenyl substituent is 1.9559(7) Å and is shorter than the Ga–C distances in **1–4** despite the increase in the gallium coordination number from two to three. This suggests even greater removal of charge density from gallium in **5**.

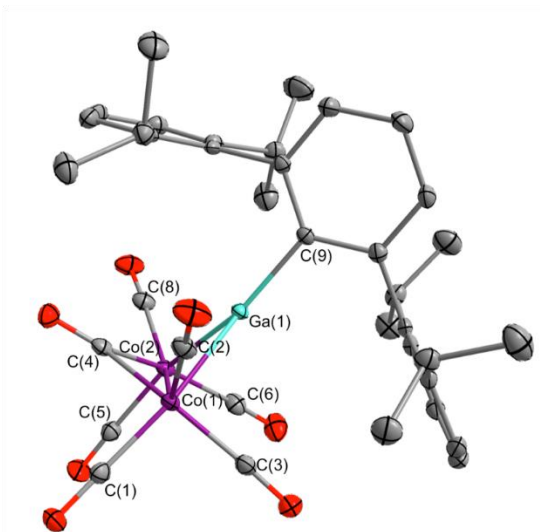


Figure 5. Thermal ellipsoid (50 %) plot of **5** with hydrogen atoms omitted for clarity. Selected bond lengths (Å) and angles (°): Co(1)–Co(2) 2.5802(4); Ga(1)–Co(1) 2.3891(3); Ga(1)–Co(2) 2.3366(3); Ga(1)–C(9) 1.9581(17); Co(1)–C(1) 1.8115(2); Co(1)–C(2) 1.7801(2); Co(1)–C(3) 1.8188(2); Co(1)–C(4) 1.9130(2); Co(2)–C(4) 1.9973(2); Co(2)–C(5) 1.8145(2); Co(2)–C(6) 1.800(2); Co(2)–C(8) 1.794(2); Co(1)–Ga(1)–C(9) 133.68(5); Co(2)–Ga(1)–C(9) 158.82(5); Co(1)–Ga(1)–Co(2) 66.173(11).

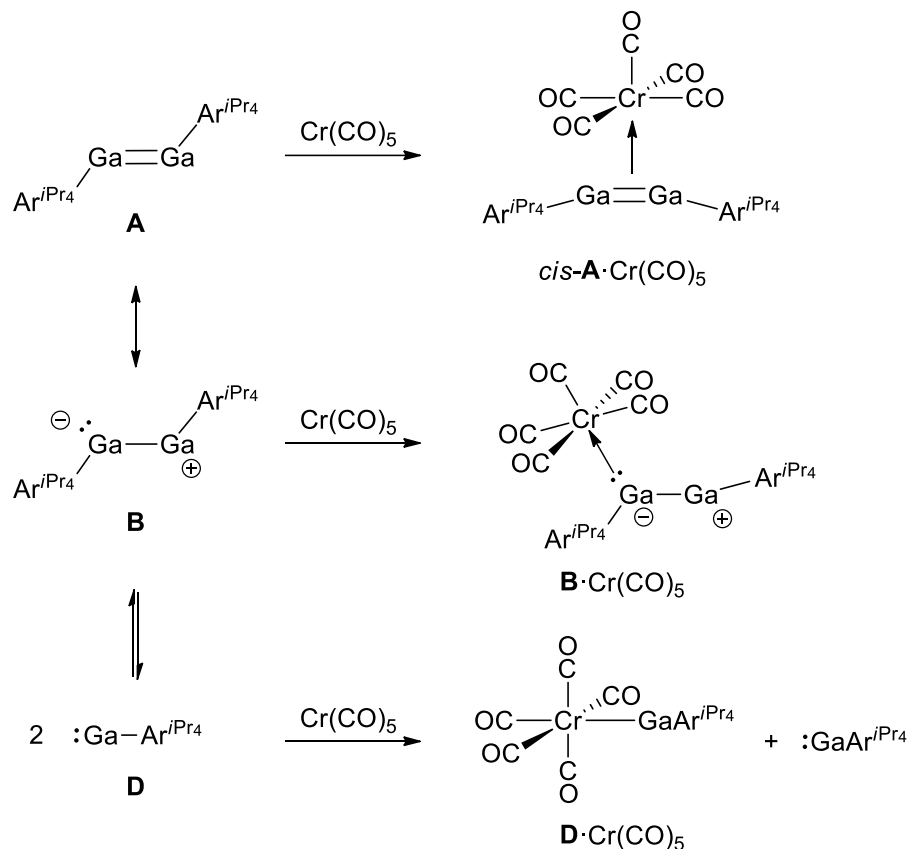
Spectroscopic data for **5** are also consistent with the monosubstituted bridging structure. The infrared spectrum of **5** shows bands in the range expected for terminal CO ligands, 2100–1850 cm^{-1} . For comparison, the complex $\text{Co}_2(\mu\text{-GaG}_{\text{iso}})_2(\text{CO})_6$ displays four CO stretching frequencies at 2031, 1992, 1955 and 1937 cm^{-1} ,^{14a} whereas those of $\text{Co}_2(\mu\text{-GaCp}^*)_2(\text{CO})_6$ are found at 2023, 1989, 1953, 1948 cm^{-1} .¹⁰ A weak band at 1835 cm^{-1} in the IR spectrum of **5** is assigned as the bridging carbonyl stretch as this matches well with the range expected for such signals, 1850–1720 cm^{-1} .

Mechanistic Calculations. While it seems clear that $:\text{GaAr}^{i\text{Pr}_4}$ ligands are acting as Lewis basic 2-e^- fragments in the isolated products **1–3**, we first postulated that the compounds **1–3** were formed by association of one equivalent of an activated transition metal carbonyl (*i.e.* $\text{M}(\text{CO})_5$) to form a compound resembling a Lewis acid stabilized structure of type **B**. This proposal in which the digallene (**A**, **B** or **C**) rather than the monomeric gallanediyl (**D**) is the reactive species appears to be counterintuitive because

of steric considerations. However it has been shown that the activation barrier of the digallene toward olefins and hydrogen is considerably lower than that of the gallanediyl.⁵ To probe which form dictates the reactivity with metal carbonyls, optimizations of possible intermediates in the model reaction between $\text{Ar}^{i\text{Pr}_4}\text{GaGaAr}^{i\text{Pr}_4}$ and $\text{Cr}(\text{CO})_6$ were performed using density functional theory (DFT).

Given the high stability of $\text{Cr}(\text{CO})_6$ with respect to ligand association²² and the spectroscopic evidence that, under photolysis in solution, the $\text{Cr}(\text{CO})_5$ fragment reacts rapidly with σ -donors prior to further CO dissociation,²³ the formation of **1–3** is unlikely to involve intermediates in which chromium is either seven- or four-coordinate. Therefore, the Ga–Cr bond forming step of this reaction is likely to involve association of $\text{Cr}(\text{CO})_5$ with a gallium species of the type **A**, **B** or **D**. Because of the very small contribution of diradical character (form **C**) to the structure of digallenes and the observation that addition of a Lewis acid would further stabilize resonance form **B**,⁶ the possibility for a diradical reaction mechanism was not considered.

The proposed mechanisms for the Ga–Cr bond-forming step are shown in Scheme 2. Optimization of each of the three possible intermediates immediately revealed that the complex **B**· $\text{Cr}(\text{CO})_5$ is not a stable minimum on the potential energy surface despite the minimal change in conformation required for Ga–Cr bond formation. In fact, all geometry optimizations of **B**· $\text{Cr}(\text{CO})_5$ resulted in barrierless cleavage of the Ga–Ga bond to form **D**· $\text{Cr}(\text{CO})_5$ and $:\text{GaAr}^{i\text{Pr}_4}$. This implies that the Ga–Cr bond formation takes place at the expense of the Ga–Ga bond and that a weakly bound **B**· $\text{Cr}(\text{CO})_5$ does not represent a stable (characterizable) intermediate. In contrast, the complex **D**· $\text{Cr}(\text{CO})_5$ was found to be stable and form readily via simultaneous optimization of the gallanediyl ligand **D** and $\text{Cr}(\text{CO})_5$. Its ready formation is supported by the synthesis and structure of its molybdenum analogue **4**.



Scheme 2. Possible Ga–Cr bond forming steps in the reaction of Cr(CO)_6 and $\text{Ar}^{i\text{Pr}}_4\text{GaGaAr}^{i\text{Pr}}_4$.

For both steric and electronic reasons, Cr(CO)_5 was found to form a stable interaction that bridges both gallium atoms only when **A** is in a nearly planar *cis*-conformation. Given the significant steric strain associated with adopting this geometry, it is not surprising that *cis-A*· Cr(CO)_5 is much higher in energy than **D**· Cr(CO)_5 + $\text{:GaAr}^{i\text{Pr}}_4$ (156 kJ mol^{-1}). What is unusual, however, is the significant shortening of the Ga–Ga bond in this species, from 2.640 \AA in the optimized structure of $\text{Ar}^{i\text{Pr}}_4\text{GaGaAr}^{i\text{Pr}}_4$ to 2.405 \AA in *cis-A*· Cr(CO)_5 . This phenomenon contrasts with the notion of digallenes behaving as heavy element alkene analogues since alkene binding at transition metals is normally associated with lengthening of the C–C bond.

To rationalize the above observations, a molecular orbital (MO) analysis of the fragments involved in each of these species was performed. The relevant frontier orbitals are displayed in Figure 6. It is immediately evident that there is no symmetry allowed combination of frontier orbitals between *trans*-Ar^{iPr}₄GaGaAr^{iPr}₄ and Cr(CO)₅ that would result in binding of the transition metal fragment at both gallium centers. However, the interaction of the HOMO of *cis*-A and the LUMO of Cr(CO)₅ is symmetry allowed, and the resulting HOMO of *cis*-A·Cr(CO)₅ is the only occupied frontier orbital that has a significant contribution affecting the Ga–Ga bond. This readily explains the unusual contraction of this bond upon complexation by transition metal stabilization of a homoatomic group 13 π-bond, a phenomenon observed recently via the synthesis of a related diborene complex.²⁴ However, the strengthening of the Ga–Ga bond as well as the relative thermodynamic instability of a *cis*-A·Cr(CO)₅ species with respect to **D**·Cr(CO)₅ suggest that it is not a viable intermediate in the formation of **1–3**.

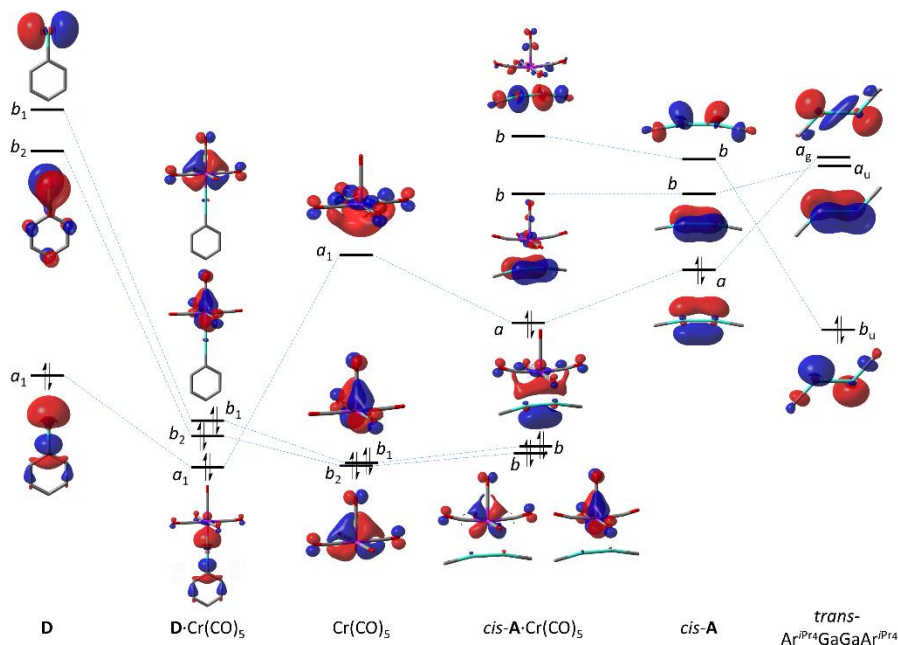
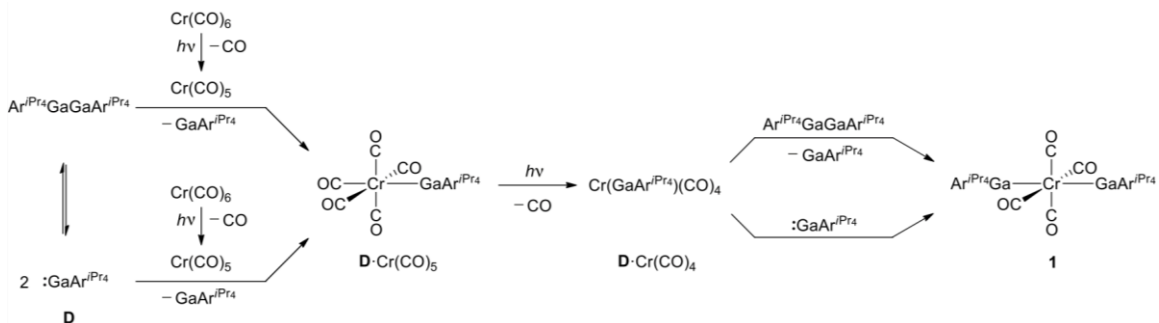


Figure 6. Frontier molecular orbitals of the proposed intermediates involved in Ga–Cr bond formation. For clarity, the Ar^{iPr}₄ unit in digallene-containing species is omitted (with the exception of the ipso carbon) along with the hydrogen atoms and 2,6-(C₆H₃-2,6-ⁱPr₂)₂ substituents of gallanediyls. Orbital symmetries have been assigned based on the symmetry of the respective molecule or molecular fragment.

The molecular orbital analysis supports the intermediacy of **D**·Cr(CO)₅ in the formation of **1–3**. The complex **D**·Cr(CO)₅ is stabilized primarily by a σ -type interaction involving the HOMO of the gallanediyl and the LUMO of the Cr(CO)₅ fragment, giving the HOMO–2 of the complex. The other occupied frontier orbitals of **D**·Cr(CO)₅ (HOMO and HOMO–1) show only very minor polarization of the chromium d-orbitals towards gallium, in agreement with the spectroscopic data indicating weak π -acceptor nature of the gallanediyl ligands also in **1–3**.

Finally, the spontaneous dissociation of :GaAr^{iPr₄} from **B**·Cr(CO)₅ can be understood based on a comparison between the HOMO of *trans*-Ar^{iPr₄}GaGaAr^{iPr₄} and LUMO+1 of *cis*-Ar^{iPr₄}GaGaAr^{iPr₄} (Figure 6). Upon complexation by Cr(CO)₅, sterics enforce a shift toward linear geometry for the uncomplexed, two-coordinate gallium. The increasing σ^* character of the formerly b_u -symmetric HOMO destabilizes the Ga–Ga interaction and results in bond cleavage. Thus, the addition of a Lewis acidic metal complex to Ar^{iPr₄}GaGaAr^{iPr₄} will likely result in the generation of a :GaAr^{iPr₄} adduct unless the Ga–Ga bond can be stabilized, for example, via interaction of an additional Lewis base.

Taken together, the computational results show that the photochemical reaction of Ar^{iPr₄}GaGaAr^{iPr₄} with Cr(CO)₆ most likely proceeds via an intermediate Cr(GaAr^{iPr₄})(CO)₅ complex. Since previous experiments have revealed that an equilibrium between monomeric :GaAr^{iPr₄} and dimeric Ar^{iPr₄}GaGaAr^{iPr₄} exists in solution,² it is likely that Cr(CO)₅ reacts competitively with both species in the initial Ga–Cr bond forming step. While modeling of the reaction between Cr(GaAr^{iPr₄})(CO)₅ and Ar^{iPr₄}GaGaAr^{iPr₄} was not performed due to the computational cost involved, the similarity of the electronic structures of **D**·Cr(CO)₅ and Cr(CO)₆, and the relative simplicity of this reaction step implicate an analogous mechanism for the formation of the second Ga–Cr bond. Thus, photolytic cleavage of one CO molecule to give an intermediate **D**·Cr(CO)₄ followed by addition of :GaAr^{iPr₄} (possibly competitively with the dimer Ar^{iPr₄}GaGaAr^{iPr₄}) would yield disubstituted **1** (Scheme 3).



Scheme 3. Suggested mechanism for the photochemical reaction of Cr(CO)_6 and $\text{Ar}^{i\text{Pr}}_4\text{GaGaAr}^{i\text{Pr}}_4$.

CONCLUSIONS

We have shown that the digallene $\text{Ar}^{i\text{Pr}}_4\text{GaGaAr}^{i\text{Pr}}_4$ undergoes a photochemical reaction with activated transition metal carbonyl fragments to form complexes where two CO ligands are replaced by $\text{:GaAr}^{i\text{Pr}}_4$. The IR stretching frequencies of the CO ligands indicate that the $\text{:GaAr}^{i\text{Pr}}_4$ ligand is a good σ -donor and a poor π -acceptor. Density functional theory calculations show that the reaction with Cr(CO)_6 likely proceeds via the monosubstituted $\text{Cr(GaAr}^{i\text{Pr}}_4\text{)(CO)}_5$, formed when the photoactivated Cr(CO)_5 fragment reacts competitively with the gallanediyl $\text{:GaAr}^{i\text{Pr}}_4$ and the digallene $\text{Ar}^{i\text{Pr}}_4\text{GaGaAr}^{i\text{Pr}}_4$. The formation of $\text{Cr(GaAr}^{i\text{Pr}}_4\text{)(CO)}_5$ is supported by the synthesis of $\text{Mo(GaAr}^{i\text{Pr}}_4\text{)(CO)}_5$. The reactivity was also rationalized from a molecular orbital perspective, which indicated only a fleeting existence for adducts of $\text{Ar}^{i\text{Pr}}_4\text{GaGaAr}^{i\text{Pr}}_4$ with Lewis acidic metal fragments in the absence of a Lewis base. The reactivity of the digallene $\text{Ar}^{i\text{Pr}}_4\text{GaGaAr}^{i\text{Pr}}_4$ with transition metal carbonyls presents further evidence for the lability of the Ga–Ga bond.

EXPERIMENTAL SECTION

General Considerations. All manipulations were performed under anaerobic and anhydrous conditions using Schlenk techniques and a Vacuum Atmospheres drybox. The digallene $\text{Ar}^{i\text{Pr}_4}\text{GaGaAr}^{i\text{Pr}_4}$ was synthesized by a literature procedure.^{2c} The hexacarbonyls $\text{M}(\text{CO})_6$ ($\text{M} = \text{Cr}, \text{Mo}, \text{W}$) and $\text{Co}_2(\text{CO})_8$ were purchased commercially and used as received. $\text{Mo}(\text{CO})_5\text{NMe}_3$ was prepared by a literature procedure.³² Solvents were dried and stored over sodium. Physical measurements were obtained under anaerobic and anhydrous conditions. ^1H and $^{13}\text{C}\{^1\text{H}\}$ NMR spectra were collected on a Varian spectrometer and referenced to known standards. IR spectra were recorded as Nujol mulls between CsI plates on a Perkin-Elmer 1430 spectrometer. UV-visible spectra were recorded as dilute hexane or chloroform solutions in 3.5 mL quartz cuvettes using an Olis 17 Modernized Cary 14 UV/Vis/NIR spectrophotometer. Melting points were determined on a Meltemp II apparatus using glass capillaries sealed with vacuum grease and are uncorrected.

General Synthetic Procedure for 1–3: $\text{Ar}^{i\text{Pr}_4}\text{GaGaAr}^{i\text{Pr}_4}$ (0.10 g, 0.11 mmol) and 1 equivalent (0.11 mmol) of $\text{M}(\text{CO})_6$ ($\text{M} = \text{Cr}, \text{Mo}, \text{W}$) were dissolved in dry, degassed pentane (20 mL) in a quartz Schlenk tube under N_2 . The solution was irradiated for 3 h with a Rayonet-200 photoreactor with a wavelength range of 253–570 nm at approximately 35 W. A color change from dark green to either red or yellow was observed. As the solution cooled, crystals suitable for single crystal X-ray diffraction were formed on the tube walls. The remaining solution was decanted and concentrated under reduced pressure to *ca.* 5 mL then stored at -18°C which afforded additional crystals of *trans*- $[\text{M}(\text{GaAr}^{i\text{Pr}_4})_2(\text{CO})_4]$.

1: *trans*- $[\text{Cr}(\text{GaAr}^{i\text{Pr}_4})_2(\text{CO})_4]$: Red crystals. Yield: 26 %. m.p. 338–342°C (dec). λ_{max} in hexane (ϵ): 243 nm ($6.0 \times 10^3 \text{ L mol}^{-1} \text{ cm}^{-1}$), 314 nm ($8.6 \times 10^2 \text{ L mol}^{-1} \text{ cm}^{-1}$), 380 nm ($1.2 \times 10^3 \text{ L mol}^{-1} \text{ cm}^{-1}$). IR, cm^{-1} (Nujol mull): 2924 (w), 2854 (w), 1894 (s). ^1H NMR (400 MHz, C_6D_6 , 298 K): 1.03 (d, *o*- $\text{CH}(\text{CH}_3)_2$, $^2J_{\text{HH}} = 6.8 \text{ Hz}$, 12H), 1.39 (d, *o*- $\text{CH}(\text{CH}_3)_2$, $^2J_{\text{HH}} = 6.8 \text{ Hz}$, 12H), 2.91 (sept, *o*- $\text{CH}(\text{CH}_3)_2$, $^2J_{\text{HH}} = 6.8 \text{ Hz}$, 4H), 6.99 (d, Ar, 4H), 7.06 (t, Ar, 2H), 7.24 (d, 8H), 7.38 (t, Ar, 4H). $^{13}\text{C}\{^1\text{H}\}$ NMR (C_6D_6 , 150.6 MHz, 298 K): 23.9, 24.8, 30.8, 106.1, 123.9, 129.6, 137.3, 144.2, 147.0, 164.2, 220.5.

2: *trans*-[Mo(GaAr^{iPr4})₂(CO)₄]: Yellow crystals. Yield: 15 %. m.p. 260–262°C (dec). λ_{max} in CHCl₃ (ϵ): 360 nm (1.5×10^3 L mol⁻¹ cm⁻¹), 395 nm (7.5×10^2 L mol⁻¹ cm⁻¹). IR, cm⁻¹ (Nujol mull): 2952 (w), 1904 (s). ¹H NMR (400 MHz, C₆D₆, 298 K): 1.05 (d, *o*-CH(CH₃)₂, ³J_{HH} = 6.8 Hz, 12H), 1.38 (d, *o*-CH(CH₃)₂, ³J_{HH} = 6.8 Hz, 12H), 2.92 (sept, *o*-CH(CH₃)₂, ³J_{HH} = 6.8 Hz, 4H), 7.01 (d, Ar, ³J_{HH} = 7.6 Hz, 4H), 7.10 (t, Ar, ³J_{HH} = 7.6 Hz, 2H), 7.24 (d, Ar, ³J_{HH} = 7.6 Hz, 8H), 7.35 (t, Ar, ³J_{HH} = 7.6 Hz, 4H). ¹³C{¹H} NMR (C₆D₆, 150.6 MHz, 298 K): 24.0, 24.9, 31.0, 124.0, 129.8, 137.2, 144.5, 147.4, 165.0, 211.1.

3: *trans*-[W(GaAr^{iPr4})₂(CO)₄]: Yellow crystals. Yield: 22 %. m.p. 290–295°C (dec). λ_{max} in hexane (ϵ): 266 nm (1.9×10^4 L mol⁻¹ cm⁻¹), 288 nm (1.8×10^4 L mol⁻¹ cm⁻¹), 314 nm (1.3×10^4 L mol⁻¹ cm⁻¹), 354 nm (6.1×10^3 L mol⁻¹ cm⁻¹). IR, cm⁻¹ (Nujol mull): 2957 (w), 2873 (w), 1928 (s). ¹H NMR (600 MHz, C₆D₆, 298 K): 1.04 (d, *o*-CH(CH₃)₂, ²J_{HH} = 6.8 Hz, 12H), 1.31 (d, *o*-CH(CH₃)₂, ²J_{HH} = 6.8 Hz, 12H), 2.83 (sept, *o*-CH(CH₃)₂, ²J_{HH} = 6.8 Hz, 4H), 7.04 (d, Ar, 4H), 7.13 (t, Ar, 2H), 7.20 (d, 8H), 7.30 (t, Ar, 4H). ¹³C{¹H} NMR (C₆D₆, 150.6 MHz, 298 K): 24.0, 24.9, 31.0, 124.3, 129.8, 130.2, 136.6, 144.8, 147.6, 164.6, 196.2.

4: Mo(GaAr^{iPr4})(CO)₅: To a green solution of Ar^{iPr4}GaGaAr^{iPr4} (0.440 g, 0.566 mmol) in THF (20 mL) was added a yellow solution of Mo(CO)₅NMe₃ (0.333 g, 1.133 mmol) in THF (20 mL) dropwise at -78°C. The solution faded to yellow as and the reaction was allowed to slowly warm to room temperature overnight. The solvent was removed under reduced pressure and the residue dissolved in PhMe (50 mL). The solution was filtered using a filter tipped cannula and concentrated to *ca.* 5 mL to induce crystallization suitable for X-Ray diffraction yielding pale yellow crystals of **4**. Yield 0.240 g, 31 %, m.p. 173°C (dec). λ_{max} in hexane (ϵ): 314 nm (9800 L mol⁻¹ cm⁻¹). IR, cm⁻¹ (Nujol mull): 2070 (s), 1995 (s). ¹H NMR (600 MHz, C₆D₆, 298 K): 1.00 (d, *o*-CH(CH₃)₂, ²J_{HH} = 6 Hz, 12H), 1.27 (d, *o*-CH(CH₃)₂, ²J_{HH} = 6 Hz, 12H), 2.80 (sept, *o*-CH(CH₃)₂, ²J_{HH} = 6 Hz, 4H), 7.04–7.08 (m, Ar, 6H) 7.16 (d, Ar, ²J_{HH} = 6 Hz, 2H) 7.26 (m, Ar, 3H). ¹³C{¹H} NMR (150 MHz, C₆D₆, 298K): 23.7, 24.5, 30.5, 122.5, 123.8, 127.9, 129.7, 147.2, 200.6, 205.9.

5: Co₂(μ -GaAr^{iPr4})(μ -CO)(CO)₆: Ar^{iPr4}GaGaAr^{iPr4} (0.28 g, 0.32 mmol) and Co₂(CO)₈ (0.05 g, 0.16 mmol) were dissolved in dry, degassed THF (20 mL) in a Schlenk tube under N₂ and stirred at room temperature for 2 h. A color change from dark green to

yellow was observed. The solution was concentrated under reduced pressure and stored at *ca.* -18°C for 2 days. X-ray quality crystals formed on the sides of the flask. The remaining solution was decanted and concentrated under reduced pressure to 5 mL then stored at *ca.* -18°C to afford additional yellow crystals of $\text{Co}_2(\mu\text{-GaAr}^{i\text{Pr}_4})(\mu\text{-CO})(\text{CO})_6$. Yield: 0.04 g, 32 %. m.p. 254°C (dec). λ_{max} in hexane (ϵ): 297 nm ($3.7 \times 10^3 \text{ L mol}^{-1} \text{ cm}^{-1}$), 398 nm ($2.4 \times 10^3 \text{ L mol}^{-1} \text{ cm}^{-1}$). IR, cm^{-1} (Nujol mull): 3061 (m), 2964 (w), 2047 (w), 2010 (m), 1980 (m), 1966 (s), 1952 (s), 1927 (m), 1835 (w). ^1H NMR (400 MHz, C_6D_6 , 298 K): 0.94 (d, *o*- $\text{CH}(\text{CH}_3)_2$, $^2J_{\text{HH}} = 4 \text{ Hz}$, 12H), 1.34 (d, *o*- $\text{CH}(\text{CH}_3)_2$, $^2J_{\text{HH}} = 4 \text{ Hz}$, 12H), 2.90 (sept, *o*- $\text{CH}(\text{CH}_3)_2$, $^2J_{\text{HH}} = 4 \text{ Hz}$, 4H), 7.09–7.18 (m, Ar, 6H), 7.24 (m, Ar, 3H). $^{13}\text{C}\{^1\text{H}\}$ NMR (125 MHz, C_6D_6 , 298K): 22.6, 26.1, 30.4, 124.0, 129.2, 129.9, 138.0, 145.6, 146.8, 206.3.

X-Ray Crystallography. Crystals of **1–5** suitable for single crystal X-ray diffraction studies were covered in silicone oil and attached to a glass fiber on the mounting pin on the goniometer. Crystallographic measurements were made by using a Bruker APEX II CCD diffractometer at -183°C . The crystal structures were corrected for Lorentz and polarization effects with SAINT²⁵ and absorption using Blessing's method as incorporated into the program SADABS.²⁶ The SHELXTL program was used to determine the space groups and set up the initial files.²⁷ The structures were determined by direct methods using the program XS and refined with the program XL.²⁸ All non-hydrogen atoms were resolved anisotropically. Hydrogen atoms were placed in idealized positions throughout the refinement process.

Computational Details. Optimized geometries and vibrational frequencies were calculated with the Gaussian09 program²⁹ using spin-restricted density functional theory and the PBE0 hybrid functional.³⁰ Alrichs' triple- ζ quality basis sets (def-TZVP) were used for all atoms.³¹ Frequency calculations were performed on the located stationary points associated with reaction intermediates in order to verify that they represented true minima on the potential energy surface.

ASSOCIATED CONTENT

Supporting information

¹H NMR, ¹³C NMR, FT-IR and UV-Vis spectra of compounds 1-3 and **5**, ¹H NMR, ¹³C NMR and UV-Vis spectra for **4**.

Optimized Coordinates for Calculated Structures

Crystallographic information files for **1 – 5** (CIF)

AUTHOR INFORMATION

*E-mail: heikki.m.tuononen@jyu.fi.

*E-mail: pppower@ucdavis.edu.

Notes

The authors declare no competing financial interest

ACKNOWLEDGEMENTS

P.P.P. thanks the U.S. Department of Energy (DE-FG02-07ER46475) for support of this work. H.M.T acknowledges support from the Academy of Finland (projects 136929, 253907, and 272900) and the University of Jyväskylä. This work was also supported in part by the NSF Graduate Research Opportunities Worldwide Program (C.J.R). CSC - the IT Center for Science in Finland is thanked for CPU time.

REFERENCES

- 1 Caputo, C. A.; Power, P. P. *Organometallics*, **2013**, *32*, 2278.
- 2 (a) Zhu, Z.; Fischer, R. C.; Ellis, B. D.; Rivard, E.; Merrill, W. A.; Olmstead, M. M.; Power, P. P.; Guo, J.-D.; Nagase, S.; Pu, L. *Chem. Eur. J.*, **2009**, *15*, 5263. (b) Hardman, N. J.; Wright, R. J.; Phillips, A. D.; Power, P. P. *J. Am. Chem. Soc.*, **2003**, *125*, 2667. (c) Hardman, N. J.; Wright, R. J.; Phillips, A. D.; Power, P. P. *Angew. Chem. Int. Ed.*, **2002**, *41*, 2842.
- 3 Caputo, C. A.; Zhu, Z.; Brown, Z. D.; Fettingner, J. C.; Power, P. P. *Chem. Commun.*, **2011**, *47*, 7506.
- 4 Caputo, C. A.; Guo, J.-D.; Nagase, S.; Fettingner, J. C.; Power, P. P. *J. Am. Chem. Soc.*, **2012**, *134*, 7155.
- 5 Caputo, C. A.; Koivistoinen, J.; Moilanen, J.; Boynton, J. N.; Tuononen, H. M.; Power, P. P. *J. Am. Chem. Soc.*, **2013**, *135*, 1952.
- 6 Moilanen, J.; Power, P. P.; Tuononen, H. M. *Inorg. Chem.*, **2010**, *49*, 10992.
- 7 Al-Rafia, S. M. I.; Malcolm, A. C.; McDonald, R.; Ferguson, M. J.; Rivard, E. *Angew. Chem. Int. Ed.*, **2011**, *50*, 8354.
- 8 Gemel, C.; Steinke, T.; Cokoja, M.; Kempter, A.; Fischer, R. A. *Eur. J. Inorg. Chem.*, **2004**, 4161.
- 9 (a) Uddin, J.; Frenking, G. *J. Am. Chem. Soc.*, **2001**, *123*, 1683. (b) Uddin, J.; Boehme, C.; Frenking, G. *Organometallics*, **2000**, *19*, 571.
- 10 Jutzi, P.; Neumann, M. P.; Reumann, G.; Stammel, H.-G. *Organometallics*, **1998**, *17*, 1305.
- 11 Cokoja, M.; Gemel, C.; Steinke, T.; Welzl, T.; Winter, M.; Fischer, R. A. *J. Organomet. Chem.*, **2003**, *684*, 277.
- 12 Seifert, A.; Linti, G. *Inorg. Chem.*, **2008**, *47*, 11398.
- 13 Su, J.; Li, X.-W.; Crittendon, R. C.; Campana, C. F.; Robinson G. H., *Organometallics* **1997**, *16*, 4511.
- 14 (a) Jones, C.; Stasch, A.; Moxey, G. J.; Junk, P. C.; Deacon, G. B. *Eur. J. Inorg. Chem.*, **2009**, 3593. (b) Jones, C.; Mills, D. P.; Rose, R. P.; Stasch, A.; Woodul W. D. *J. Organomet. Chem.*, **2010**, *695*, 2410.
- 15 Serrano, O.; Hoppe, E.; Power, P. P. *J. Clust. Sci.*, **2010**, *21*, 449.
- 16 (a) Bach, C.; Willner, H.; Wang, C.; Rettig, S. J.; Trotter, J.; Aubke, F. *Angew. Chem., Int. Ed. Engl.*, **1996**, *35*, 1974. (b) Oldfield, E.; Keniry, M. A.; Shinoda S.; Schramm,

- S.; Broen, T.; Gutkowsky, H. S. *J. Chem. Soc., Chem. Commun.*, **1985**, 791. (c) Gleeson, J. W.; Vaughan, R. W. *J. Chem. Phys.*, **1983**, 78, 5384.
- 17 Ehlers, A. W.; Ruiz-Morales, Y.; Baerends, E. J.; Ziegler, T. *Inorg. Chem.* **1997**, 36, 5031.
- 18 Pyykkö, P.; Atsumi, M. *Chem. Eur. J.*, **2009**, 15, 186.
- 19 (a) Desclaux, J. P. *At. Dat. Nucl. Data Tables*, **1973**, 12, 311. (b) Kutzelnigg, W. *Angew. Chem., Int. Ed. Engl.*, **1984**, 23, 272. (c) Mann, J. B. *Atomic Structure Calculations II. Hartree-Fock Wave Functions and Radial Expectation Values: Hydrogen to Lawrencium*, LA-3691, Los Alamos Scientific Laboratory: Los Alamos, New Mexico, USA, 1968.
- 20 Mathieu, R.; Lenzi, M.; Poilblanc, R. *Inorg. Chem.*, **1970**, 9, 2030.
- 21 Leung, P. C.; Coppens, P. *Acta. Cryst.*, **1983**, B39, 535.
- 22 Abel, E. W.; Stone, F. G. A. *Q. Rev. Chem. Soc.*, **1970**, 24, 498
- 23 Welch, J. A.; Peters, K. S.; Vaida, V. *J. Phys. Chem.*, **1982**, 86, 1941.
- 24 Braunschweig, H.; Damme, A.; Dewhurst, R. D.; Vargas, A. *Nat. Chem.*, **2013**, 5, 115.
- 25 Bruker *SMART APEX (2013.6-2) and SAINT (2009 Version 7.68s)*, Bruker AXS Inc.: Madison, Wisconsin, USA, 2009 and 2013.
- 26 (a) Sheldrick, G. M. *SADABS 'Siemens Area Detector Absorption Correction'*, Universität Göttingen: Göttingen, Germany, 2012/1. (b) Blessing, R. H. *Acta Cryst. A*, **1995**, 51, 33.
- 27 Sheldrick, G. M. *SHELXTL* Version 6.1; Bruker AXS Inc.: Madison, Wisconsin, USA, 2000.
- 28 Sheldrick, G. M. *Acta Cryst.*, **2008**, A64, 112.
- 29 Gaussian 09, Revision D.01, M. J. Frisch, G. W. Trucks, H. B. Schlegel, G. E. Scuseria, M. A. Robb, J. R. Cheeseman, G. Scalmani, V. Barone, B. Mennucci, G. A. Petersson, H. Nakatsuji, M. Caricato, X. Li, H. P. Hratchian, A. F. Izmaylov, J. Bloino, G. Zheng, J. L. Sonnenberg, M. Hada, M. Ehara, K. Toyota, R. Fukuda, J. Hasegawa, M. Ishida, T. Nakajima, Y. Honda, O. Kitao, H. Nakai, T. Vreven, J. A. Jr. Montgomery, J. E. Peralta, F. Ogliaro, M. Bearpark, J. J. Heyd, E. Brothers, K. N. Kudin, V. N. Staroverov, R. Kobayashi, J. Normand, K. Raghavachari, A. Rendell, J. C. Burant, S. S. Iyengar, J. Tomasi, M. Cossi, N. Rega, M. J. Millam, M. Klene, J. E. Knox, J. B. Cross, V. Bakken, C. Adamo, J. Jaramillo, R. Gomperts, R. E. Stratmann, O. Yazyev, A. J. Austin, R. Cammi, C. Pomelli, J. W. Ochterski, R. L. Martin, K. Morokuma, V. G. Zakrzewski, G. A. Voth, P. Salvador, J. J. Dannenberg, S. Dapprich, A. D. Daniels, Ö. Farkas, J. B. Foresman, J. V. Ortiz, J. Cioslowski, D. J. Fox, Gaussian, Inc.: Wallingford, Connecticut, USA, 2009.

- 30 (a) Perdew, J. P.; Burke, K.; Ernzerhof, M. *Phys. Rev. Lett.*, **1996**, *77*, 3865. (b) Perdew, J. P.; Ernzerhof, M.; Burke, K. *J. Chem. Phys.*, **1996**, *105*, 9982. (c) Perdew, J. P.; Burke, K.; Ernzerhof, M. *Phys. Rev. Lett.*, **1997**, *78*, 1396. (d) Adamo, C.; Barone, V. *J. Chem. Phys.*, **1999**, *110*, 6158.
- 31 (a) Schaefer, A.; Huber, C.; Ahlrichs, R. *J. Chem. Phys.*, **1994**, *100*, 5829. (b) Andrae, D.; Haeussermann, U.; Dolg, M.; Stoll, H.; Preuss, H. *Theor. Chim. Acta* **1990**, *77*, 123.
- 32 Maher, J. M.; Beatty, R. P.; Cooper, N. J. *Organometallics*, **1985**, *4*, 1354.